Dissolution kinetics of nanoscale liquid Pb/Bi inclusions at a grain boundary in aluminum

Sergei I. Prokofjev · Erik Johnson ·
Victor M. Zhilin · Ulrich Dahmen

Abstract In situ transmission electron microscopy is used to study dissolution of liquid single-phase Pb/Bi inclusions attached to a grain boundary in an alloy of $Al_{99.29}Pb_{0.65}Bi_{0.06}$ at temperatures of 343, 370, and 389 °C, respectively. The initial size of the inclusions was smaller than 60 nm. Dissolution of the inclusions was observed until their complete disappearance. Digitized video recordings of the process of dissolution were used to obtain the dependence of the inclusion size with time. The kinetics of the dissolution of the grain boundary inclusions can be described with a model where it is assumed that grain-boundary diffusion of Pb and Bi is the controlling mechanism. The high value (2.3 eV) of the apparent activation enthalpy of dissolution indicates that the process is likely governed by the large negative enthalpies of solubility of Pb and Bi in Al.

S. I. Prokofjev (✉) · V. M. Zhilin
Institute of Solid State Physics, Russian Academy of Sciences,
142432 Chernogolovka, Moscow District, Russia
e-mail: prokof@issp.ac.ru

S. I. Prokofjev · E. Johnson
Nano Science Center, Niels Bohr Institute, University
of Copenhagen, Universitetsparken 5, 2100 Copenhagen Ø,
Denmark

E. Johnson
Materials Research Department, Risø National Laboratory,
Technical University of Denmark, 4000 Roskilde, Denmark

U. Dahmen
National Center for Electron Microscopy, Lawrence Berkeley
National Laboratory, Berkeley, CA 94720, USA

Introduction

Inclusions of a second phase (solid and liquid precipitates, gas bubbles, pores, and so on) attached to grain boundaries in multiphase materials can have a strong influence on the kinetics of grain-boundary processes, such as grain-boundary migration, grain-boundary sliding, creep, etc. [1–3]. These processes are important for development of particular microstructures, the rate at which they evolve or degrade and, consequently, the service properties and the lifetime of engineering materials. They are related to the density of inclusions on grain boundaries, their size distributions, their morphologies, and the kinetics by which they change size [1, 2]. It is therefore important to study the microscopic kinetic mechanisms that contribute to the evolution of a system of grain-boundary inclusions.

Theoretical models for coarsening of grain-boundary inclusions, which is controlled by grain-boundary diffusion [4, 5], show that the average size r of inclusions in an ensemble approximately follows the law $r^4 - r_o^4 \propto t$, where r_o is the initial average size of the inclusions and t is the elapsed time. However, several experiments show that the dependence of the average size as a function of time is rather $r^n - r_o^n \propto t$, where the power n may vary from 3 to 5 [6–9]. This was attributed to contributions from grain-boundary diffusion, bulk diffusion [10, 11], and dislocation pipe diffusion [5, 12] to a total diffusion solute transfer.

In addition, growth and dissolution of inclusions during coarsening may also be controlled by diffusion mechanisms related to the transfer of matrix material or by attachment (detachment) of matrix atoms to (from) the matrix crystal lattice at the inclusion surface [13]. A number of mechanisms can therefore participate simultaneously to a coarsening process that will depend on temperature and inclusion sizes. Hence, it may not be possible to associate

unambiguously the kinetic behavior with a single mechanism. Therefore, examination of the (growth) dissolution of individual inclusions in a simple system during well-defined conditions is expected to provide better information on the mechanisms controlling them.

In the present article, an attempt of such a study is presented. Dissolution of individual nanoscale liquid Pb/Bi inclusions attached to a grain boundary in a thin Al foil was investigated using in situ TEM. The kinetics of the dissolution process of the inclusions was measured using digitized images from real time video sequences providing a high accuracy due to good time resolution, image contrast, and relatively high rates of dissolution.

Experimental

The samples used in our study were prepared from ribbons of an alloy of Al with 0.65 at. % Pb and 0.06 at. % Bi, obtained by rapid solidification from a temperature above the Al–Pb liquid immiscibility gap by the melt-spinning technique. The as-processed microstructure of the samples consisted of dense distributions of nanosized Pb/Bi inclusions embedded in the grains of the polycrystalline Al matrix and with larger inclusions attached to grain boundaries.

In situ TEM observations of the kinetics of the dissolution of grain-boundary inclusions were carried out in a 200 kV Philips CM 20 microscope using a single-tilt heating stage (Gatan) at temperatures of 343, 370, and 389 °C, where the inclusions are expected to be single-phase according to the Al–Bi, Al–Pb, and Bi–Pb phase diagrams [14]. The observations were recorded on video (25 frames/s). The accuracy of the sample temperature control was around 1 K. The error in the absolute temperature determination is estimated to be around 5–10 K.

TEM observations

TEM observations show that liquid Pb/Bi inclusions attached to grain boundaries gradually shrink in size until they become completely and irreversibly dissolved. In contrast, intragranular inclusions in the matrix, both free and attached to dislocations, did not display any size change during the duration of the experiments and at the temperatures used, which is in agreement with earlier observations [15]. Figure 1 shows a set of frames taken from a video sequence of the experiment recorded at 343 °C where the Pb/Bi grain-boundary inclusions are melted. It demonstrates clearly how in situ TEM observations can be used to monitor shrinkage and dissolution of the liquid Pb/Bi grain-boundary inclusions.

The grain-boundary inclusions shown in Fig. 1 have a visually smooth lens shape without any visible facets. The large axis of the grain-boundary inclusions has been used as a measure of their size, and it is assumed to be equal to the diameter d of the circular cross section between the lens-shaped inclusions and the grain-boundary plane.

Results

The results of the video analyses are presented in Fig. 2, which shows the size of the liquid grain-boundary inclusions as a function of time for temperatures 343, 370, and 389 °C, respectively. The graphs show a notable scatter of data-points that is primarily due to noise in the individual video frames, thus limiting the accuracy of the size measurement. This effect is likely to become stronger as the inclusions shrink in size and may therefore lead to a systematic error in the size versus time plots for the smallest sizes.

Analysis of results

Reduction of the total interfacial energy of an ensemble of inclusions of a second phase is the driving force of the coarsening process. As the smaller inclusions dissolve, the larger inclusions grow in size. The kinetics of coarsening of an ensemble of grain-boundary inclusions controlled by grain-boundary diffusion was considered theoretically in [4, 5]. In contrast, we observe complete dissolution of all grain-boundary inclusions, Fig. 1. This is believed to be due to the presence of the free surfaces of the TEM foils, since accumulation of the second phase on the free surfaces can lead to a decrease in the total free energy of the system. Then, a driving force causing irreversible diffusion transfer of second-phase material from grain-boundary inclusions to a surface is expected as the interface between superficial second phase and matrix is flat.

In the following model, we consider dissolution of an isolated grain-boundary inclusion with the geometry shown in Fig. 3. For simplicity, we consider a grain boundary of finite size in the shape of a circular disk with radius R with the inclusion of radius r located at the center. In relation to the in situ TEM experiment, we also assume that $R = L/2$, where L is the distance between the free foil surfaces measured along the plane of the grain boundary. The shape of the grain-boundary inclusion is assumed to be a lens consisting of two similar spherical caps joined at their bases. It is assumed that the grain-boundary inclusion interacts only with the layer of the second phase on each of the free surfaces of the TEM foil, which we have taken to be equivalent to an inclusion of infinite radius. Then, the
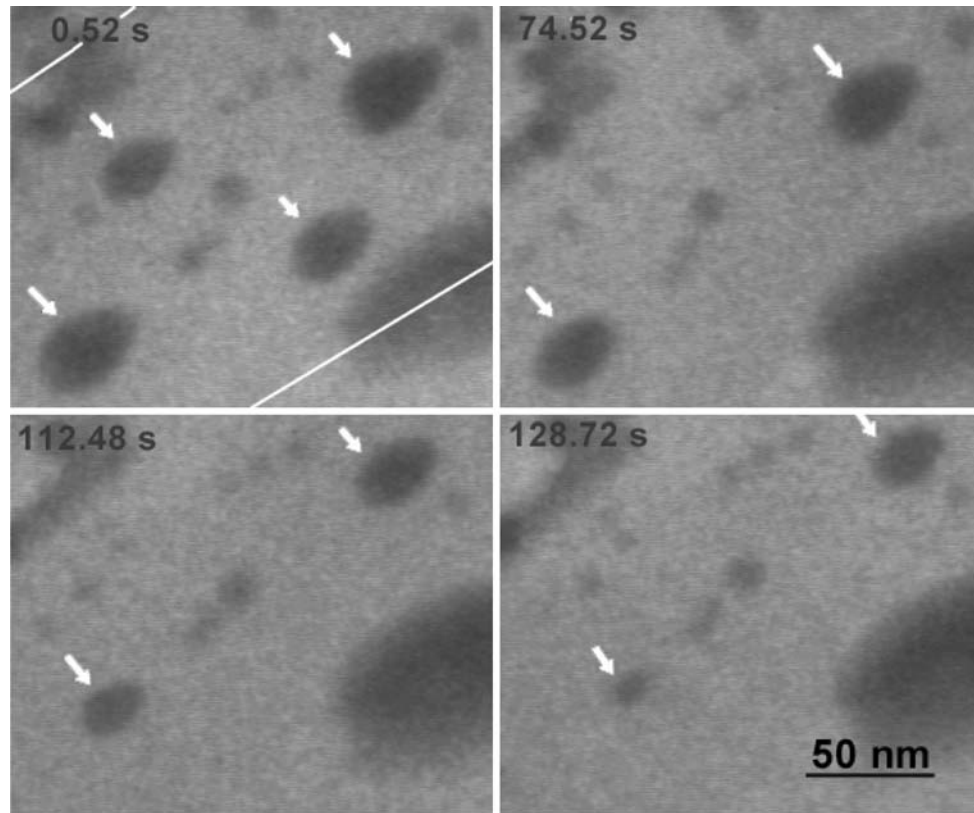
Fig. 1 Four frames from a video sequence illustrating in situ TEM observation of dissolution of liquid Pb/Bi inclusions located on a grain boundary in an Al matrix at 343 °C. In order to get the clearest images from the inclusions the sample is oriented to minimize diffraction effects from the grain boundary. The *arrows* indicate liquid Pb/Bi grain-boundary inclusions, which have a characteristic lens shape. The *white lines* outline the approximate limits of the projection of the grain boundary on the image plane. Small rounded inclusions whose sizes do not change during the experiment are intragranular matrix inclusions overlapping the projection of the grain boundary
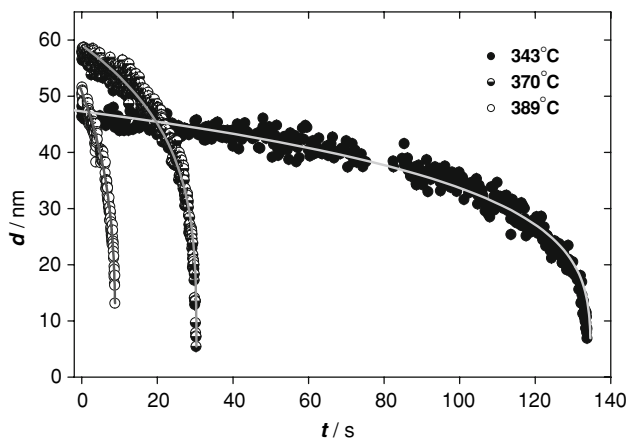

Fig. 2 The size dependence of the liquid Pb/Bi grain-boundary inclusions as a function of time for three different temperatures 343, 370, and 389 °C measured from individual frames of the video sequences. The *lines* present the fits to Eq. 2 (see the text below). Each dataset represents measurements on one inclusion

Fig. 3 Model used for the mathematical analysis of the dissolution of grain-boundary liquid Pb/Bi inclusions in Al. All notations used are explained in the text

grain-boundary concentration of solute near the free surface is equal to its equilibrium grain-boundary concentration. In the exper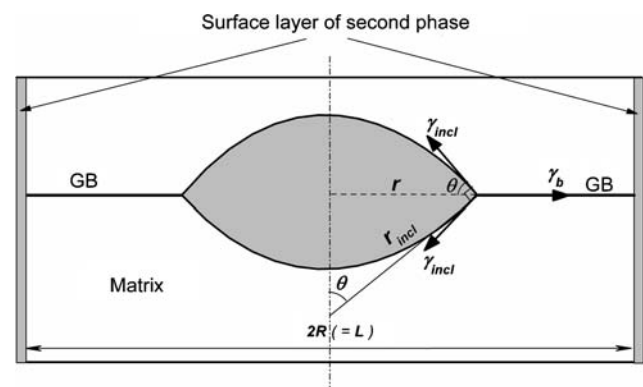iments, some of the grain-boundary inclusions in the TEM foils are closer to each other than to one of the free surfaces of the foil. However, as the inclusion sizes are all of the same order of magnitude, the influence of neighboring inclusions is much smaller than the influence from the free surfaces which are equivalent to infinitely large inclusions, i.e., the concentration gradient between
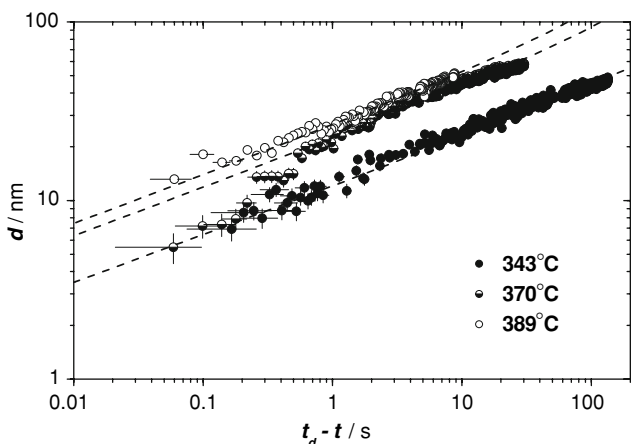
Fig. 4 The size dependence of the liquid Pb/Bi grain-boundary inclusions as a function of time (see Fig. 2) re-plotted in $\log(d)$ versus $\log(t_d - t)$ coordinates. The *dashed lines* represent fits to Eq. 2
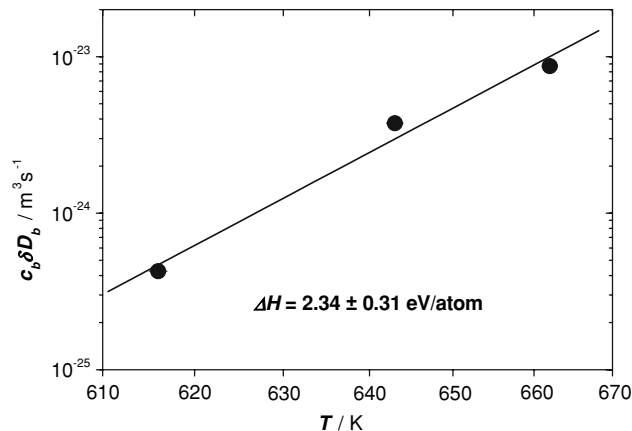

Fig. 5 Arrhenius dependence of the term $Q = c_b \delta D_b$. The *solid line* presents the fit to the Arrhenius dependence. The apparent activation enthalpy for dissolution obtained from the fit is indicated

neighboring inclusions is smaller than the concentration gradients between the inclusions and the free surfaces.

The mathematical analysis similar to that carried out in [4, 5] leads to the following rate equation for the decrease as a function of time t in the radius r of the grain-boundary inclusion

$$\frac{dr}{dt} = -\frac{2\gamma_{incl}\Omega c_b \delta D_b}{\beta k T r^3 \ln(L/2r)}, \tag{1}$$

where γ_{incl} is the surface tension of inclusion/matrix interface, c_b is the equilibrium molar concentration of solute in the grain boundary, δ is the diffusion thickness of the grain boundary, D_b is the grain-boundary diffusion coefficient of solute, Ω is the atomic volume of the solute, T is the temperature (K), and k is the Boltzmann constant, $\beta = (2 - 3\cos\theta + \cos^3\theta)/\sin^4\theta$, where θ is the dihedral angle (see Fig. 3) determined by the relationship $\cos\theta = \gamma_b/2\gamma_{incl}$ (γ_b is the surface tension of the grain boundary). Taking $2r = d$ and $2r_o = d_o$, the solution of Eq. 1 can be written as

$$\left(\frac{d}{d_o}\right)^4 \left[\frac{\ln(L/d) + 1/4}{\ln(L/d_o) + 1/4}\right] = 1 - \frac{t}{t_d}, \tag{2}$$

where

$$t_d = \frac{\beta k T d_o^4 [\ln(L/d_o) + 1/4]}{128\gamma_{incl}\Omega c_b \delta D_b} \tag{3}$$

is the time required for complete dissolution (the lifetime) of an inclusion of initial size d_o.

Using t_d values obtained from the size versus time plots in Fig. 2, the data are re-plotted in $\log(d)$ versus $\log(t_d - t)$ coordinates in Fig. 4. The fits of the data to Eq. 2 are shown as *solid lines* in Fig. 2 and as *dashed lines* in Fig. 4. In the fitting procedure, we used a value of $L = 150$ nm.

However, due to the logarithmic terms containing L in Eq. 2, a change in the value of L will have little influence on the results. Figure 4 shows that the fits between Eq. 2 and the experimental data match fairly well except for the smallest inclusion sizes, e.g., for t close to t_d, and that dissolution of the inclusions is therefore adequately described by Eq. 2.

From Eq. 3, the term $Q = c_b \delta D_b$ was calculated at 343, 370, and 389 °C using d_o and t_d obtained from the kinetic plots in Fig. 2. For the calculations we used $\gamma_{incl} = 300$ mJ/m², $\Omega = 3.14 \cdot 10^{-29}$ m³, $L = 1.5 \cdot 10^{-7}$ m, and $\beta \cong 1.15$, which was estimated using $\theta \approx 62°$ obtained from measurements of the dihedral angle 2θ on the large inclusion at the triple point where it joins with the grain boundary. Note that the angle is close to $\theta \approx 63.6°$ obtained from similar measurements of grain-boundary Pb inclusion in Al matrix at 460 °C [16]. The Arrhenius dependence of $c_b \delta D_b$ is shown in Fig. 5. The apparent activation enthalpy obtained is 2.34 ± 0.31 eV.

Discussion

The term Q can be written as $Q = sc\delta D_b$, where $s = c_b/c$ is the coefficient of grain-boundary segregation, and c is the molar concentration of Pb/Bi in the bulk solution. According to the Al–Bi and Al–Pb phase diagrams [14], at the temperatures of the experiment a saturated solution of Al in liquid Pb/Bi, which is the material of "the Pb/Bi inclusions," is in equilibrium with a saturated solution of Pb/Bi in solid Al, which is the material of the "Al matrix." Then, a grain-boundary solution of Pb/Bi (away from the Pb/Bi inclusions) is expected to be saturated as it is in equilibrium with the saturated bulk solution. Therefore, $c = c^{sat}$ and $c_b = c_b^{sat}$, where c^{sat} and c_b^{sat} are the bulk and

grain-boundary solubilities of Pb/Bi in Al, respectively, at the given temperature. So, in our case $s = c_b^{sat}/c^{sat1} = s^{sat}$.

Taking $D_b = D_{bo} \exp(-\Delta H_{diff}/kT)$, $c^{sat} = c_o^{sat} \exp(\Delta H_{sol}/kT)$, and $s^{sat} = s_o^{sat} \exp(-\Delta H_{segr}^{sat}/kT)$, the temperature dependence of Q can be written as $Q = s_o^{sat} c_o^{sat} \delta D_{bo} \exp[-\Delta H/kT]$, where $\Delta H = \Delta H_{segr}^{sat} - \Delta H_{sol} + \Delta H_{diff}$ is the apparent activation enthalpy of the dissolution process. Here, ΔH_{segr}^{sat} is the apparent enthalpy of grain-boundary segregation in the saturation case, ΔH_{diff} is the activation enthalpy of grain-boundary diffusion, ΔH_{sol} is the solubility enthalpy, and the multipliers s_o^{sat}, c_o^{sat}, and D_{bo} are the corresponding pre-exponential factors.

The isotherm of grain-boundary segregation in the case of restricted bulk and grain-boundary solubilities is described by the expression

$$X_b = \frac{X \exp(-\Delta G_{segr}/kT)}{1 - X + X \exp(-\Delta G_{segr}/kT)}, \qquad (4)$$

where $X = c/c^{sat}$, $X_b = c_b/c_b^{sat}$, and ΔG_{segr} is the segregation free energy [3]. An apparent segregation free energy ΔG_{segr}^{app} can be defined as $X_b/X = \exp(-\Delta G_{segr}^{app}/kT)$. Then, according to Eq. 4, ΔG_{segr}^{app} will approach zero, when the bulk solute concentration approaches saturation as $s^{sat} = x_b^{sat}/x^{sat} = 1$. Therefore, $\Delta G_{segr}^{app} = \Delta G_{segr}^{sat} \equiv 0$ at $x = x^{sat} = 1$ at all temperatures along the *soludus* line. Hence, the apparent segregation enthalpy ΔH_{segr}^{sat} corresponding to ΔG_{segr}^{sat} is $\Delta H_{segr}^{sat} \equiv 0$ at $x = x^{sat} = 1$ giving $\Delta H = -\Delta H_{sol} + \Delta H_{diff}$.

Data on grain-boundary diffusion of Pb and Bi in Al are absent, so a value of $\Delta H_{diff} = 0.8$ eV for grain-boundary self-diffusion in Al is estimated using the empirical relationship $\Delta H_{diff} = 83T_m$ J/mol proposed for grain-boundary self-diffusion in fcc metals [17]. That gives a rough estimate of ΔH_{diff} for grain-boundary diffusion of Pb and Bi in Al. Ab initio calculations give $\Delta H_{sol} = -1.56$ eV for Pb in Al, and $\Delta H_{sol} = -1.61$ eV for Bi in Al [18]. Thus, we obtain an estimate of the dissolution enthalpy of $\Delta H \approx 2.4$ eV that agrees well with $\Delta H = 2.34$ eV obtained experimentally. Such a close agreement seems to be rather fortuitous because the accuracy of the data used for the estimate is most likely

not that high. Nevertheless, the estimate gives a good indication that the large apparent activation enthalpy of the dissolution of grain-boundary liquid Pb/Bi inclusions in Al is due to the contribution of the large negative enthalpies of the Pb and Bi solubilities in Al.

Summary

- Kinetics of dissolution of individual small (<60 nm) liquid single-phase Pb/Bi inclusions attached to a grain boundary in an Al matrix is studied at 343, 370, and 389 °C using in situ TEM. Sizes of the inclusions as a function of time were measured on individual video frames obtained from real-time video sequences. The kinetic behavior of the change in inclusion size with time was analyzed using a simple model, where an inclusion was assumed to interact only with the liquid Pb/Bi layer on the sample surfaces, whose effect is set equal to that of an inclusion of infinite size.

- The kinetics of dissolution of liquid Pb/Bi grain-boundary inclusions in an Al matrix can be described well enough from the assumption that grain-boundary diffusion is the controlling mechanism.

- It is shown that the high value (2.34 eV) of the apparent activation enthalpy of the dissolution process is due to the large negative magnitudes of the enthalpy of solubility of Pb (-1.56 eV) and Bi (-1.61 eV) in Al.

---

¹ It can be written that $c_b^{sat}/c^{sat} = (c_{bo}^{sat}/c_o^{sat}) \exp[(\Delta H_b^{sol} - \Delta H^{sol})/RT]$, where ΔH_b^{sol} and ΔH^{sol} are the solute solubility enthalpies in grain-boundary and bulk solutions, respectively. The chemical potentials of the same component atoms in saturated bulk and grain-boundary solutions, which are in equilibrium are related as $\mu_b^{sat} = \mu^{sat} + \bar{A}_{sol}\gamma_b^{sat}$, where $\bar{A}_{sol}$ is the partial molar area of solute in grain boundary, and γ_b^{sat} (0.3 J/m) is the surface tension of a grain boundary saturated with the solute. Then, one can show that $\Delta H_b^{sol} - \Delta H^{sol} = \bar{A}_{sol}\gamma_b^{sat} \cong \Omega_{matr}\gamma_b^{sat}/\delta \approx 10$ kJ/mol $\ll \Delta H^{sol}$, where δ ($0.5 \cdot 10^{-9}$ m) is the width of a grain boundary. Indeed, when the solute solubility in a grain boundary is restricted, the partial molar area can be defined as $\bar{A}_{sol} = A_m + (1 - X_b)\partial A_m/\partial X_b$, where $A_m = \Omega_m/\delta = [\Omega_{matr}(1 - c_b) + \Omega_{sol}c_b]/\delta$ is the molar grain boundary area, $X_b = c_b/c_b^{sat}$, Ω_{matr} ($2 \cdot 10^{-5}$ m³) and Ω_{sol} are the molar volumes of matrix and solute atoms, respectively. So, one can show that $\bar{A}_{sol} = [\Omega_{matr}(1 - c_b^{sat}) + c_b^{sat}\Omega_{sol}]/\delta \cong \Omega_{matr}/\delta$ if $c_b^{sat} \ll 1$.

References

1. Geguzin YaE, Krivoglaz MA (1973) Migration of macroscopic inclusions in solids. Consultants Bureau, New York
2. Ashby MF (1980) Recrystallization and grain growth of multi-phase and particle containing materials. In: Hansen N, Jones AR, Leffers T (eds) First Risø international symposium on metallurgy and materials science, Risø National Laboratory, Roskilde, p 325
3. Gottstein G, Shvindlerman LS (1999) Grain boundary migration in metals. CRC Press, Boca Raton
4. Speight MV (1968) Acta Metall 16:133
5. Ardell AJ (1972) Acta Metall 20:601
6. Butler EP, Swann PR (1976) Acta Metall 24:343
7. Czurratis P, Kroggel P, Löffler H (1988) Z Metallkd 79:307
8. Fujii T, Moriyama M, Kato M, Mori T (1993) Philos Mag 68:137
9. Monzen R, Hasegawa T (1997) Philos Mag Lett 76:69
10. Lifshitz IM, Slyozov VV (1961) J Phys Chem Solids 19:35
11. Wagner C (1961) Z Electrochem 65:581

12. Kreye H (1970) Z Metallkd 61:108
13. Sun W (2005) Acta Mater 53:3329
14. Massalski TB (Ed.-in-Chief) (1986) Binary alloy phase diagrams, vol 1. ASM, Metals Park, OH, pp 96, 147, 524
15. Gabrisch H, Kjeldgaard L, Johnson E, Dahmen U (2001) Acta Mater 49:4259
16. Gabrisch H, Dahmen U, Johnson E (1998) Microsc Res Tech 42:241
17. Kaur I, Gust W (1988) Fundamentals of grain and interphase boundary diffusion. Ziegler, Stuttgart
18. Wolverton C, Ozoliņš V (2006) Phys Rev B73:144104